**517 Wide field retinal imaging**
Thursday, May 11, 2017 8:30 AM–10:15 AM
Exhibit/Poster Hall Poster Session
**Program #/Board # Range:** 5445–5459/B0602–B0616
**Organizing Section:** Multidisciplinary Ophthalmic Imaging Group

**Program Number:** 5445 **Poster Board Number:** B0602
**Presentation Time:** 8:30 AM–10:15 AM
**Evolution of vitreoretinal separation in normal subjects as described by wide-angle montage imaging of optical coherence tomography**
*Mayuka Tsukahara[1], Keiko Mori[1], Peter L. Gehlbach[2], Keisuke Mori[1].*
[1]Department of Ophthalmology, International University of Health and Welfare, Nasu-Shiobara, Tochigi, Japan; [2]Department of Ophthalmology, Johns Hopkins University, Baltimore, MD.
**Purpose:** Posterior vitreous detachment (PVD) plays an important role in several vitreoretinal interface disorders. Historically, observations of PVD using optical coherence tomography (OCT) were limited to the macular region. The purpose of this study is to describe the morphology of the vitreoretinal interface, from the macula to the periphery, in normal subjects, using montaged OCT images.
**Methods:** The design of this study is a prospective, consecutive interventional case series. All investigations adhered to the tenets of the Declaration of Helsinki. Recruited were 70 healthy eyes of 50 normal subjects, ranging from 21 to 75 years (48.9 ± 18.3 [mean ± SD]). Montaged images of horizontal and vertical OCT scans through the fovea, were obtained in each subject as previously described.
**Results:** Based on the montaged OCT images, the PVD was classified into the following 5 stages: stage 0, no PVD (0 eye); stage 1, focal PVD limited to paramacular, peripheral or from paramacular to peripheral zones (48 eyes, 45.2 ± 18.5 years [mean ± SD]); stage 2, perifoveal PVD expanding to the periphery (8 eyes, 53.7 ± 14.6 years); stage 3, near-complete PVD with persistent vitreopapillary adhesion alone (2 eyes, 59.5 ± 0.5 years); stage 4, complete PVD (12 eyes, 66.7 ± 8.5 years). Initiation of vitreous separation often occurred in a superior quadrant in 94% of stage one PVDs.
**Conclusions:** Using wide-angle montage OCT we have successfully imaged the vitreoretinal interface from the macula to the periphery and documented the longitudinal development of age-related PVD. Whereas prior work suggests that PVD originates in the perifoveal region, our observations clearly demonstrate more peripheral points of initiation. Our findings also show that PVD is usually initiated superiorly but that other quadrants may also be involved. Initiation of PVD is observable even in the second decade of life, much younger than previously appreciated. Following initiation, PVDs generally progress slowly and move posteriorly to the perifoveal region and anteriorly to the periphery.

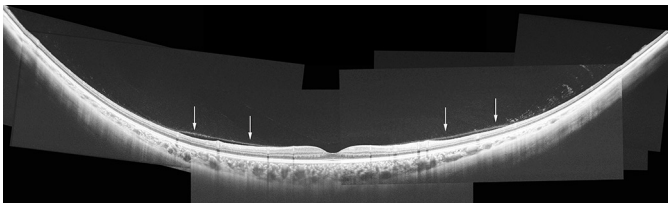

A vertical montage OCT image of 32 years old female with stage 1 PVD. Focal PVD is limited to the paramacular region (arrows).
**Commercial Relationships: Mayuka Tsukahara**, None; **Keiko Mori**, None; **Peter L. Gehlbach**, None; **Keisuke Mori**, None

**Program Number:** 5446 **Poster Board Number:** B0603
**Presentation Time:** 8:30 AM–10:15 AM
**Wide-field multimodal ophthalmic imaging using scanning laser ophthalmoscopy and optical coherence tomography at 400 kHz**
*Mohamed T. El-Haddad[1], Karen M. Joos[2], Shriji Patel[2], Yuankai Tao[1].*
[1]Biomedical Engineering, Vanderbilt University, Nashville, TN; [2]Ophthalmology and Visual Sciences, Vanderbilt University, Nashville, TN.
**Purpose:** Scanning laser ophthalmoscopy (SLO) and optical coherence tomography (OCT) enable *in vivo* imaging of ophthalmic structures. Multimodality SLO-OCT systems provide complementary *en face* and cross-sectional information for aiming, bulk motion registration, and multi-field mosaicking. We previously demonstrated a swept-source spectrally-encoded SLO and OCT (SS-SESLO-OCT) system using single-mode illumination and multimode collection through a double-clad fiber coupler to improve collection efficiency and reduce speckle contrast. Here, we present a novel SS-SESLO-OCT system for wide-field imaging at 400 kHz line-rate.
**Methods:** SESLO and OCT illumination and optical triggering and clocking used a shared 1060 nm Axsun swept-source optically buffered to 400 kHz. SESLO and OCT images were acquired simultaneously on a dual-channel digitizer with a combined throughput of 2.4 GS/s using shared imaging optics and digitization, triggering, and clocking electronics (Fig. 1(a), (b)).
**Results:** *In vivo* ophthalmic imaging was performed in a healthy volunteer under an IRB-approved protocol. Corneal (Fig. 1(c)-(e)) and widefield retinal (Fig. 1(f)-(h)) images were sampled at 2560 x 2000 pix. (spectral x lateral) with 1400 frames-per-volume at 200 frames-per-second. A full *en face* SESLO frame was acquired simultaneously with each OCT cross-section. Multimode collection provided >3x increase in collection efficiency and >3.5x reduction in speckle contrast.
**Conclusions:** SS-SESLO-OCT enables high-speed multimodal widefield imaging of ocular structures. Simultaneous *en face* and cross-sectional imaging provides complementary information that may be used for image aiming, retinal tracking, and multi-volumetric registration, averaging, and mosaicking.

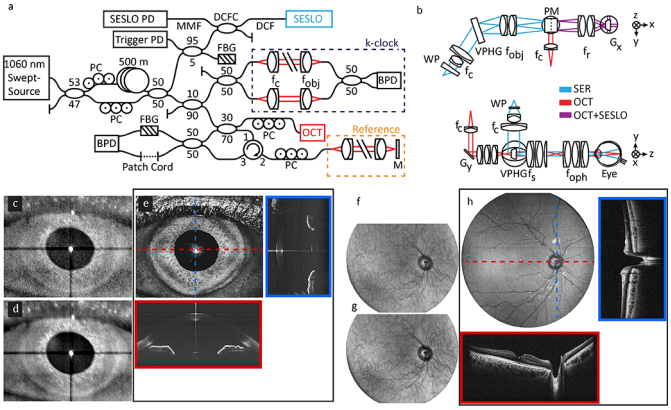


Fig.1. *In vivo* corneal and retinal imaging using SS-SESLO-OCT. (a) SS-SESLO-OCT illumination and detection engine and (b) imaging relay. (c), (f) Single-frame and (d), (g) 5-frame averaged SESLO images. (e), (h) *En face* and cross-sectional OCT images. DCF, double-clad fiber; FBG, fiber Bragg grating; f, collimating, objective, ophthalmic, relay, and scan lenses; $G_{x,y}$, galvanometer scanners; M, mirror; MMF, multimode fiber; PC, polarization controller; BPD, balanced photodiode; PM, prism mirror; VPHG, grating; WP, wedge prism.

**Commercial Relationships: Mohamed T. El-Haddad**; **Karen M. Joos**, None; **Shriji Patel**, None; **Yuankai Tao**, Leica Microsystems (P), Cleveland Clinic Foundation (P), Leica Microsystems (R)

**Program Number:** 5447 **Poster Board Number:** B0604
**Presentation Time:** 8:30 AM–10:15 AM
**Ultra-wide field optical coherence tomography angiography for evaluation of diabetic retinopathy**
*Qinqin Zhang[1], Chieh-Li Chen[1], Zhongdi Chu[1], Kasra Attaran-Rezaei[2], Ruikang K. Wang[1]*. [1]Department of Bioengineering, University of Washington, Seattle, WA; [2]Department of ophthalmology, Seattle, WA.
**Purpose:** To develop ultra-wide field OCT angiography (UW-OCTA) for imaging patients with diabetic retinopathy (DR)
**Methods:** UW-OCTA was developed based on a 1060 nm swept source OCTA engine (Plex Elite, Carl Zeiss Meditec. Inc) running at 100 kHz A-line rate with motion tracking mechanism. A montage scanning protocol was designed to enable the UW-OCTA imaging, covering a field of view (FOV) of ~100 degrees. For the montaging scan, 16 cube scans were performed on each patient. Each cube scan covered 6mm×6mm sampled by 500 A-lines × 500 B-frames with 2 repetitions at each B-scan location. Complex OMAG algorithm was used to extract blood flow information. To visualize retinal vasculature, three layers were segmented including vitreous retinal layer (VRL) covering a slab 100 microns above the ILM, superficial retinal layer (SRL) extending from ILM to IPL, deep retinal layer (DRL) from outer border of IPL to outer border of OPL, which were then color-coded to appreciate depth information. Longitudinal scans of DR patients were collected before and after laser/anti-VEGF treatment to show the usefulness of the UW-OCTA in the clinical imaging of DR patients
**Results:** 3 patients with DR including non-proliferative diabetic retinopathy and proliferative diabetic retinopathy underwent UW-OCTA images before and after laser/anti-VEGF treatment. In comparison with FA, UW-OCTA images provide distinct and detailed visualization of vascular networks over ~100-degree FOV. The neovasculatures located in the peripheral VRL were precisely detected and these neovessels were regressed dramatically after anti-VEGF treatment. The UW-OCTA images showed the macular ischemia and non-perfusion regions in far peripheral region at one scope, which makes it possible to quantify vascular features within all 7 defined EDTRS fields. UW-OCTA images also provided detail information of other vascular features, including microaneurysms and intra-retinal microvascular abnormalities (IRMA), and their locations
**Conclusions:** The wide angle OCTA is capable of imaging peripheral retina, comparable with wide-angle fundus image. We have successfully demonstrated the UW-OCTA of DR patients that extends to more than 100-degree view angle, and provides unprecedented vascular details in the peripheral regions. Further studies will be done to quantify OCTA defined by standard EDTRS and find the role in treatment of different macular diseases

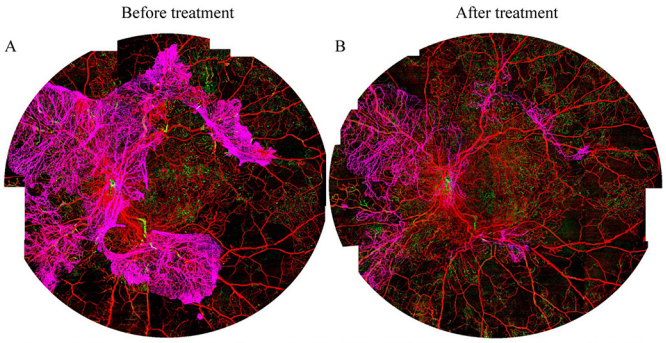

Figure 1 29 years old female diagnosed with PDR. UW-OCTA images of the patient (A) before treatment and (B) one month follow-up visit after anti-VEGF treatment. The neovascular in VRL (purple) was suppressed dramatically after anti-VEGF treatment. Macular ischemia and non-perfusion area was observed in the peripheral region as dark regions in the enface angiograms. Color-coded images offers depth information. Purple represents VRL. Red represents SRL. Green represents DRL. The FOV of UW-OCTA images is ~ 100 degrees.

**Commercial Relationships: Qinqin Zhang**, None; **Chieh-Li Chen**, None; **Zhongdi Chu**, None; **Kasra Attaran-Rezaei**, None; **Ruikang K. Wang**, Carl Zeiss Meditec. Inc (C), Carl Zeiss Meditec. Inc (P), Carl Zeiss Meditec. Inc (R), Carl Zeiss Meditec. Inc (F)

**Program Number:** 5448 **Poster Board Number:** B0605
**Presentation Time:** 8:30 AM–10:15 AM
**Ocular morphometry from wide-field, whole eye OCT compared to MRI and PCI**
*Ryan P. McNabb[1], Robin R. Vann[1], Joseph A. Izatt[2, 1], Anthony N. Kuo[1, 2]*. [1]Ophthalmology, Duke University Medical Center, Durham, NC; [2]Biomedical Engineering, Duke University, Durham, NC.
**Purpose:** Ocular morphometry (or biometry) is an important part of clinical care, such as cataract surgical planning, and in research where eye shape from MRI has been correlated with pathological myopia. While widely used in ophthalmology, optical coherence tomography's use in ocular morphometry has generally been limited due to technical and optical constraints in imaging the eye as a whole. We describe here the development of a "whole eye" OCT system that overcomes these constraints to simultaneously image full views of the anterior chamber and 50° on the retina (macula + optic nerve) and provide ocular morphometry.
**Methods:** A tabletop 200kHz swept source ($\lambda_0$=1045nm; Axsun, Inc.) OCT system with a polarization encoded, dual channel sample arm was developed to simultaneously image both the anterior and posterior eye in a single volume (Fig. A-E). Four subjects (N = 8 eyes) were consented under an IRB approved protocol to have "whole eye" OCT volumes, and for comparison, also have PCI (LenStar, Haag-Streit) and MRI (1mm T1; MR 750 3.0 T, GE, Inc.). For morphometric analysis, OCT images were segmented, corrected for subject and system optical distortions, and oriented correctly in a virtual space (Fig. F). Retinal curvature (*R*c) and axial length (*AL*) from OCT were compared to MRI and PCI respectively. Non-parametric Wilcoxon sign rank test was used for statistical analysis.
**Results:** Curvature measured by whole eye OCT (*R*c= 11.49±0.59mm) compared to MRI (*R*c= 11.11±0.33mm) was not statistically significantly different ($\Delta R$c = -0.38±0.62mm, $p$ = 0.219). Axial length measured by whole eye OCT (*AL* = 23.13±0.87mm) compared to PCI (*AL* = 23.19±0.76mm) was also not statistically different ($\Delta AL$ = 0.063±0.288, $p$ = 0.557).
**Conclusions:** We demonstrated a wide-field, whole eye OCT system capable of simultaneously providing quantitative morphometric analysis of ocular tissue within a single volume acquisition that is not statistically significantly different from MRI and PCI. This has

important clinical implications for OCT as a complete platform to both examine layered microstructure and for ocular morphometry analysis.

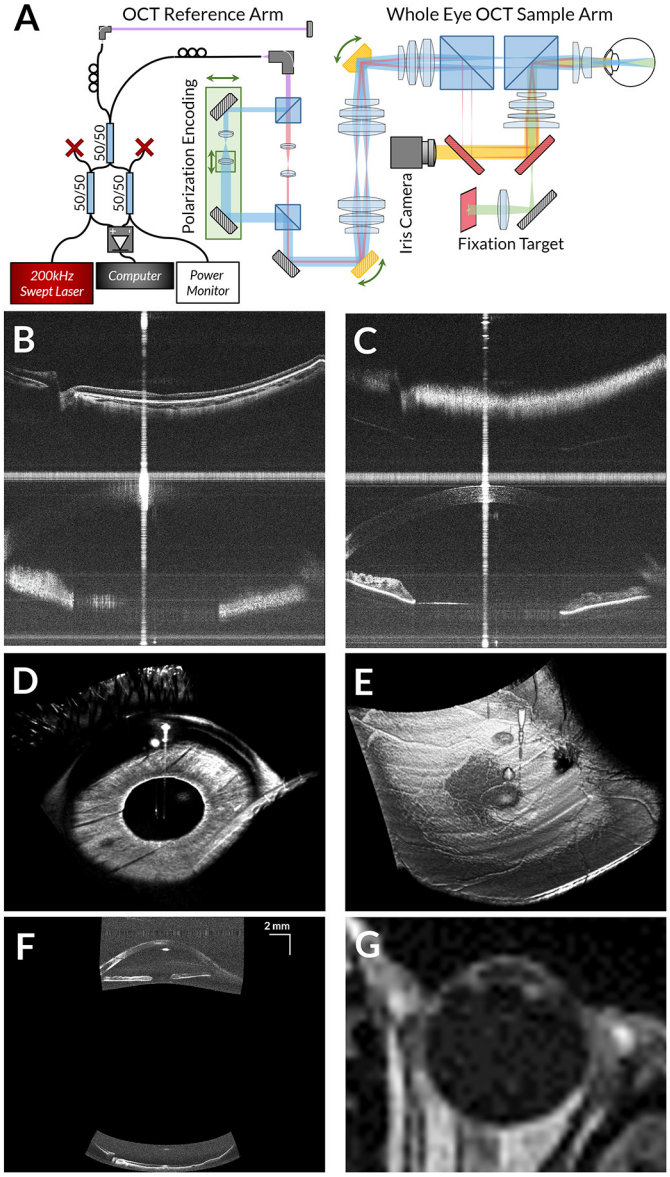


*A)* Whole eye OCT imaging system schematic *B&C)* Averaged B-scan dispersion corrected for posterior and anterior segment respectively *D&E)* Simultaneously acquired volumes of anterior and posterior segment *F)* Whole eye OCT B-scan distortion corrected for morphological analysis *G)* T1 MRI cross-section of same eye as *F* for comparison

**Commercial Relationships: Ryan P. McNabb**, None; **Robin R. Vann**, None; **Joseph A. Izatt**, Leica Microsystems (P), Leica Microsystems (R); **Anthony N. Kuo**, None

**Support:** NIH R01-EY024312 and NIH R01-EY023039

**Program Number:** 5449 **Poster Board Number:** B0606
**Presentation Time:** 8:30 AM–10:15 AM

## Usability of Widefield Slit-Scanning Ophthalmoscopes for Fundus Autofluorescence Imaging

*Mary K. Durbin, Jennifer Luu, Conor Leahy, Robert Sprowl, T K. Brock*. R & D, Carl Zeiss Meditec, Inc, Dublin, CA.

**Purpose:** To demonstrate the usability of fundus autofluorescence (FAF) images acquired using a prototype widefield (WF) slit-scanning ophthalmoscope (SSO) (ZEISS, Dublin, CA), imaging over a 90° field of view (FOV) as measured from the cornea.
**Methods:** A prototype WF SSO was used to acquire 90° FAF images on 8 undilated eyes from 6 subjects with and without ocular disease, as well as True Color images for comparison. FAF is dye-less fluorescence imaging using either blue (FAF-Blue) or green (FAF-Green) illumination, which captures the natural autofluorescence of lipofuscin that accumulates in the retinal pigment epithelium (RPE). Image quality was evaluated by a licensed optometrist. Images were graded as unusable if image artifacts disrupted the ability to evaluate the central 45 degree field of view.
**Results:** Of the 16 non-mydriatic FAF images acquired, 81% (13/16) were usable. The 19% (3/16) of unusable FAF images occurred because the subjects' pupil diameters were smaller than 2.5mm, the system's limit. FAF-Blue, FAF-Green, and True Color images, each spanning a 90° FOV, are presented for a subject with a history of trauma in the left eye secondary to a car accident and status post multiple ocular surgeries (Figure 1). Both FAF images show an area of hypofluorescence superior to the optic disc, corresponding to a region of dead RPE cells. This area is not seen on the True Color image as True Color imaging does not provide functional information on the status of RPE cells. An area of peripapillary atrophy encircling the optic disc can be seen in the True Color image, and a corresponding region of hypofluorescence is present in both FAF images. Finally, accumulation of lipofuscin can be seen in the region inferior nasal to the macula as an area of hyperfluorescence in both FAF-Blue and FAF-Green images.
**Conclusions:** The prototype widefield slit-scanning ophthalmoscope is capable of acquiring 90° FAF-Blue and FAF-Green images on undilated eyes. These images provide functional information regarding the presence of dead RPE cells, missing RPE cells, and the accumulation of lipofuscin.

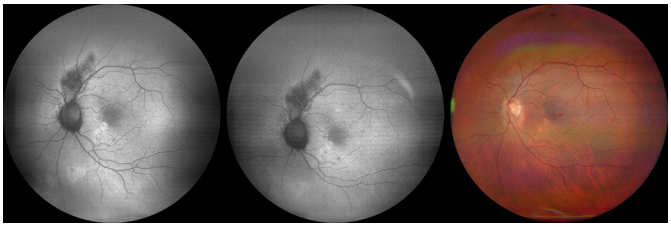

Widefield (90°) slit-scanning ophthalmoscope FAF-Blue, FAF-Green, and True Color images of the the undilated left eye of a 63 year old male with a history of ocular trauma secondary to a car accident and status post multiple ocular surgeries.

**Commercial Relationships: Mary K. Durbin**, Carl Zeiss Meditec, Inc. (E); **Jennifer Luu**, Carl Zeiss Meditec, Inc. (E); **Conor Leahy**, Carl Zeiss Meditec, Inc. (E); **Robert Sprowl**, Carl Zeiss Meditec, Inc. (E); **T K. Brock**, Carl Zeiss Meditec, Inc. (E)

**Program Number:** 5450 **Poster Board Number:** B0607
**Presentation Time:** 8:30 AM–10:15 AM
**Impact of Ultrawide Field Retinal Imaging (UWFI) on the Rapid Assessment of Avoidable Blindness and Diabetic Retinopathy(RAAB-DR) Survey**
*Gary L. Yau[3], Paolo S. Silva[3, 2], Leo D. Cubillan[1], Karlo M. Claudio[1], Kevin M. Panggat[1], Migil G. Ledesma[1], Maria A. Villano[1], Joanne C. Macenas[1], Cloyd M. Pitoc[1], Carisa M. Paraz[1], Jennifer K. Sun[3, 2], Lloyd P. Aiello[3, 2].* [1]University of the Philippines, Philippine Eye Research Institute, Manila, Philippines; [2]Ophthalmology, Harvard Medical School, Boston, MA; [3]Beetham Eye Institute, Joslin Diabetes Center, Boston, MA.
**Purpose:** To evaluate the feasibility and benefit of implementing UWFI within the efficient and cost-effective survey method of RAAB-DR used to estimate prevalence and causes of visual impairment(VI) in Central Luzon, Philippines
**Methods:** The RAAB-DR methodology estimates the prevalence of blindness, diabetes mellitus (DM) and DR in a defined geographic area. Community clusters(N=35) each with 50 subjects >=50 yrs old were selected by probability proportionate to size sampling for entry into this cross-sectional population-based survey. Participants received visual acuity(VA) screening and VI diagnosis by a study certified ophthalmologist. Subjects were classified as having DM if they had a previous diagnosis, were receiving DM treatment or had HbA1c >=6.5%. DM subjects were further assessed for DR by dilated biomicroscopy(direct and indirect). All subjects had nonmydriatic UWFI(2 stereo 200$^{o}$ images/eye; Daytona, Optos plc, Scotland, UK). Retinal images were evaluated by Joslin Vision Network protocol at a centralized reading center. Main outcome measures were prevalence and primary causes of VI(<20/40), prevalence of DR based on UWFI, and agreement between UWFI and dilated biomicroscopy for DR severity.
**Results:** 1750 individuals were identified and 1440(82.3%) evaluated. VA was >=20/40 in 1090(75.1%). The 3 top causes of VA <20/40 were untreated cataracts(n=219,62%), refractive error(n=81,23%) and posterior segment disease(n=27,8%). UWFI was done in 1358 subjects(94.3%), with ungradable images in 22(1.6%). Non-DR posterior segment disease was identified in 341(23.7%) and DM found in 377(26.1%) subjects. DR severity distribution(by UWFI) was: no DR=69.5%, mild non-proliferative DR(NPDR)=11.1%, moderate NPDR=9.3%, severe NPDR=2.7%, proliferative DR=5.0%, DME=5.6% and ungradable=2.4%. Linear-weighted DR severity agreement between UWFI and dilated biomicroscopic exam was substantial(k=0.64,95% CI,0.56-0.72), with exact agreement in 75.8% and within 1-step in 95.4%. UWFI identified more severe disease in 17.8%.
**Conclusions:** Relatively high rates of DM and DR are found in this diverse low-to-middle income population. As the first RAAB-DR survey to use UWFI, our study demonstrates that UWFI can be readily incorporated, has substantial agreement with biomicroscopy and appears to improve the ability to identify DR and non-DR retinal disease in such population-based surveys.
**Commercial Relationships: Gary L. Yau**; **Paolo S. Silva**, Optos (F); **Leo D. Cubillan**, None; **Karlo M. Claudio**, None; **Kevin M. Panggat**, None; **Migil G. Ledesma**, None; **Maria A. Villano**, None; **Joanne C. Macenas**, None; **Cloyd M. Pitoc**, None; **Carisa M. Paraz**, None; **Jennifer K. Sun**, None; **Lloyd P. Aiello**, Optos (R), Optos (F)
**Support:** Lions International

**Program Number:** 5451 **Poster Board Number:** B0608
**Presentation Time:** 8:30 AM–10:15 AM
**Analysis of peripheral vascular staining in anterior and intermediate uveitis using ultra-widefield fluorescein angiography**
*Joon-won Kang[1], Young Suk Yu[1], Hum Chung[2], Jang Won Heo[1].* [1]Ophthalmology, Seoul National University Hospital, Seoul, Korea (the Republic of); [2]Ophthalmology, Chung-Ang University Hospital, Seoul, Korea (the Republic of).
**Purpose:** To investigate the peripheral retinal vascular staining in anterior and intermediate uveitis using ultra-widefield (UWF) fluorescein angiography (FA), and to analyze the correlation of peripheral vascular change with the inflammation of anterior chamber and vitreous.
**Methods:** We retrospectively reviewed the medical records of 37 eyes of 22 patients (age: 38.31±16.85) with anterior and intermediate uveitis (anterior uveitis: 7 patients, intermediate uveitis: 15 patients). We examined UWF FA for all patients, and included the patients with initial peripheral retinal vascular staining in UWF FA (without diffuse vasculitis, diffuse capillary leakage, and macular leakage). The eyes were categorized into two groups according to the further treatment after evaluating peripheral vascular staining: no further treatment group (group 1) and further treatment group (group 2). We compared the two groups for initial and final visual acuity, the inflammation of anterior chamber and vitreous, and the improvement of the peripheral fluorescein angiographic staining.
**Results:** Of the 22 patients, the number of group 1 was 6 (11 eyes), and the number of group 2 was 16 (26 eyes). In both groups, the visual acuity was significantly improved at final visit ($p = 0.037$, $p = 0.002$). The initial anterior chamber inflammation in group 2 was significantly more severe than that in group 1 ($p = 0.029$), but the initial anterior vitreous inflammation in group 2 was not significantly different from that in group 1 ($p = 0.387$). In group 1, peripheral vascular staining was improved in 2 eyes (18.2%), and in group 2, peripheral vascular staining was improved in 6 eyes (23.1%) ($p = 0.741$). The improvement of anterior chamber and vitreous was not correlated with the improvement of peripheral vascular staining, respectively ($p = 0.585$, $p = 0.102$). The final visual acuity was not correlated with the improvement of peripheral vascular staining ($p = 0.490$).
**Conclusions:** UWF FA is useful in detecting the peripheral retinal vascular changes, and can provide additional information in managing the uveitis. However, the peripheral vascular staining in UWF FA might not influence the treatment strategies, and it was not correlated with the degree of anterior chamber and vitreous and the final visual acuity.
**Commercial Relationships: Joon-won Kang**; **Young Suk Yu**, None; **Hum Chung**, None; **Jang Won Heo**, None

**Program Number:** 5452 **Poster Board Number:** B0609
**Presentation Time:** 8:30 AM–10:15 AM
**Assessing retinal vascular biomarkers for Alzheimer's disease using ultra-widefield imaging (UWFI)**
*Lajos Csincsik[2, 1], Erin Flynn[6], Enrico Pellegrini[3], Giorgos Papanastasiou[7], Tom MacGillivray[3, 7], Craig Ritchie[8], Tunde Peto[5, 4], Imre Lengyel[2, 1]*. [1]Ocular Biology and Therapeutics, UCL-Institute of Ophthalmology, London, United Kingdom; [2]Centre for Experimental Medicine, Queen`s University Belfast, Belfast, United Kingdom; [3]Centre for Clinical Brain Sciences, The University of Edinburgh, Edinburgh, United Kingdom; [4]Queen`s University Belfast, Belfast, United Kingdom; [5]NIHR Biomedical Research Centre, Moorfields Eye Hospital NHS Foundation Trust and UCL Institute of Ophthalmology, London, United Kingdom; [6]School of Medicine and Health Sciences, The George Washington University, Washington, DC; [7]Clinical Research Imaging Centre, University of Edinburgh, Edinburgh, United Kingdom; [8]Centre for Dementia Prevention, University of Edinburgh, Edinburgh, United Kingdom.
**Purpose:** Pathological changes in the eye have been reported in a range of neurodegenerative diseases including changes in retinal vascular parameters (RVPs). The purpose of this study was to assess whether there are measurable RVP changes associated with Alzheimer`s disease (AD) using UWFI and whether any progression related changes can be detected during a 2 year period.
**Methods:** UWFiI were acquired of 20 healthy controls (HC; (MMSE>28) and 13 participants with AD (MMSE<26) using an OPTOS TX 200 scanning laser ophthalmoscope at baseline (BL) and after a two-year follow-up (FU). The study had full local Ethical Committee approval. Images were analysed using previously developed segmentation and analysis algorithms for UWFI to measure several different RVPs including arterial and venular branching, vessel width gradient (WG), fractal dimensions (FD) of the vascular network patterns and vessel tortuosity. Analysis was carried out either on the whole image or in a circular zone (Zone C) centred on the optic disc (OD) stretching from 0.5 ODDs to 2 ODDs from the OD boundary. The image and zone was further divided into four quadrants centred on the OD. Statistical analysis was carried out in GraphPad Prism (version 7.02, 2016) using a paired and unpaired t-test where appropriate; here results with $p<0.05$ were reported.
**Results:** In total, 78 images were included in the analysis (46 HC and 32 AD). There was no significant difference in age between HC and AD (77.7±7.2 vs. 71.3±10.2; $p>0.1$). At BL there was decreased arterial FD (HC=1.3±0.02; AD=1.2±0.02; $P<0.05$) and increased arterial WG (HC=$3.86x10^{-3}$±$1.39x10^{-3}$; AD=$8.43x10^{-3}$±$1.72x10^{-3}$; $p<0.05$) at the inferior-nasal quadrant on the entire image as well as in Zone C. There was an increase in venular WG in superior-nasal quadrant (HC=$4.55x10^{-3}$±$6.03x10^{-4}$; AD=$9.93x10^{-3}$±$1.77x10^{-3}$; $p<0.01$) and also when all quadrant were considered together (HC=$5.85x10^{-3}$±$3.23x10^{-4}$; AD=$8.01x10^{-3}$±$7.08x10^{-4}$; $p<0.01$) on the entire image as well as in Zone C. From BL to FU our analysis could not detect progression in any of the RVPs.
**Conclusions:** Our preliminary data suggests that retinal vascular biomarkers measured on UWFI can distinguish between HC and AD at baseline but might not be sensitive enough to detect progression during a 2 year period. Larger participant numbers and longer FU period might be needed to detect progression of RVPs.
**Commercial Relationships: Lajos Csincsik**; **Erin Flynn**, None; **Enrico Pellegrini**, None; **Giorgos Papanastasiou**, None; **Tom MacGillivray**, None; **Craig Ritchie**, None; **Tunde Peto**, None; **Imre Lengyel**, OPTOS Plc (F)
**Support:** OPTOS Plc unrestricted grant; The Bill Brown Charitable Trust

**Program Number:** 5453 **Poster Board Number:** B0610
**Presentation Time:** 8:30 AM–10:15 AM
**Quantitative Measurement of Retinal Features on Widefield Fundus Images**
*Conor Leahy[1], Jennifer Luu[1], Abouzar Eslami[2], Gary C. Lee[1], Keith E. O'Hara[1], Mary K. Durbin[1]*. [1]R&D, Carl Zeiss Meditec Inc., Dublin, CA; [2]Carl Zeiss Meditec AG, Munich, Germany.
**Purpose:** To demonstrate quantitative distance and area measurements on the retina using widefield fundus images, and to analyze the accuracy and reliability of these measurements.
**Methods:** Widefield fundus images (true-color and fundus autofluorescence) were acquired using a prototype widefield slit-scanning ophthalmoscope (ZEISS, Dublin, CA). In widefield imaging, inherent optical distortion means that 2D fundus images cannot reproducibly encode the shapes of 3D retinal features, given that patient fixation orientation naturally varies. Without making any assumptions about the shape of the retina, 2D image pixels were mapped to 3D co-ordinates defining the corresponding rays of light emerging from the pupil. The angle between rays from retinal features, multiplied by either individualized or conventional optical magnification of the eye, gives a reproducible measure of distances. Retinal regions and features were manually traced on the images by a licensed optometrist. Their measured sizes were validated using comparative assessments obtained via optical coherence tomography (CIRRUS™ HD-OCT 5000, ZEISS, Dublin, CA). Reliability was assessed over repeat captures across different modalities and patient fixation orientations.
**Results:** Widefield distance and area measurements on retinal images are presented for healthy subjects. Figure 1 illustrates measurement of optic disc area, using five same-eye captures acquired with different fixation orientations. The apparent shape of the disc is visibly distorted per fixation. The widefield area measurement (mean±SD) was 1.94±0.07 $mm^2$. A comparable optic disc area of 1.87±0.10 $mm^2$ was obtained using optical coherence tomography. The coefficient of variation (CV) for the widefield disc area measurements was 3.6%.
**Conclusions:** Measurements on the retina can be reliably determined from widefield fundus images, despite the presence of optical distortion, by employing a suitable mapping from 2D pixels to 3D co-ordinates based on the known imaging geometry.

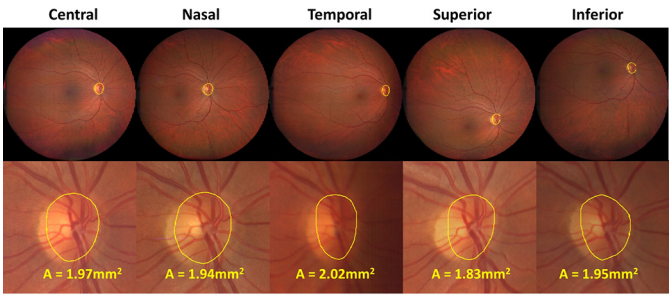


Figure 1. Widefield measurement of optic disc area using 5 same-eye captures with different fixation orientations. The CV of widefield area for the traced regions was 3.6%. The CV for the corresponding 2D enclosed image area (measured in pixels) was 15.0%, suggesting that the widefield measurement is a more reproducible assay of disc area.
**Commercial Relationships: Conor Leahy**, Carl Zeiss Meditec (E); **Jennifer Luu**, Carl Zeiss Meditec (E); **Abouzar Eslami**, Carl Zeiss Meditec (E); **Gary C. Lee**, Carl Zeiss Meditec (E); **Keith E. O'Hara**, Carl Zeiss Meditec (E); **Mary K. Durbin**, C (E)

**Program Number:** 5454 **Poster Board Number:** B0611
**Presentation Time:** 8:30 AM–10:15 AM

**Image Quality Comparison Between Non-Mydriatic and Mydriatic High-resolution True-Color Widefield Fundus Images**

*Jochen Straub, Conor Leahy, Jennifer Luu, Jeff Schmidt, Mary K. Durbin*. R&D, Carl Zeiss Meditec, Inc., Dublin, CA.

**Purpose:** To compare the color, resolution, contrast, and field of view of high-resolution true-color widefield fundus images, captured using a prototype widefield slit-scanning ophthalmoscope (ZEISS, Dublin, CA), imaging the same eyes undilated (non-mydriatic) and after dilation (mydriatic).

**Methods:** We captured high-resolution true-color widefield fundus images of the same eyes before and after dilation. We first imaged the eyes with a naturally dark-adapted pupil. After dilating the eyes using cycloplegic eye drops, we imaged the same eyes again. Pupil diameter (PD) was measured and recorded prior to each acquisition using a PD ruler. Images were visually compared by a clinical expert with respect to color, resolution, contrast, and field of view.

**Results:** We captured images on 6 eyes of 6 normal healthy subjects. The sample included eyes with natural lens (phakic) and artificial lens (pseudophakic). We were able to capture images of all eyes. Visual comparison of the images with undilated and dilated pupils showed no significant difference in color or resolution. Resolution was evaluated in the central retinal field of view and in the periphery. The achieved field of view was identical. The images captured with dilated pupils had slightly higher contrast than the images of the same eyes captured with undilated pupils. Figure 1 shows an example of an undilated eye. Figure 2 shows an image captured of the same eye after dilation.

**Conclusions:** All images taken before and after dilation were found to be clinically useful. No significant differences in color, resolution, or field of view were found when comparing non-mydriatic and mydriatic images captured with the widefield slit-scanning opthalmoscope prototype. Images of eyes with dilated pupils have slightly higher contrast. The prototype provides clinically useful true-color high-resolution widefield fundus images when imaging undilated or dilated eyes.

Fig. 1: Widefield fundus image (healthy 45 year old male; undilated; PD 3mm)

Figure 2: Widefield fundus image of the same subject (mydriatic; PD 7mm).

**Commercial Relationships: Jochen Straub**, Carl Zeiss Meditec, Inc (E); **Conor Leahy**, Carl Zeiss Meditec, Inc (E); **Jennifer Luu**, Carl Zeiss Meditec, Inc (E); **Jeff Schmidt**, Carl Zeiss Meditec, Inc (E); **Mary K. Durbin**, Carl Zeiss Meditec, Inc (E)

**Program Number:** 5455 **Poster Board Number:** B0612
**Presentation Time:** 8:30 AM–10:15 AM

## Comparison of Nonmydriatic Eye Images Acquired Using a Widefield 90° Slit-Scanning Ophthalmoscope and Standard 45° Commercial Fundus Cameras

*Jennifer Luu, Conor Leahy, Mary K. Durbin*. R&D, Carl Zeiss Meditec, Inc., Dublin, CA.

**Purpose:** Studies have shown an increase in the rate of unusable images acquired by standard commercial nonmydriatic fundus cameras for subjects >50 years of age. This study compares the quality and field of view (FOV) of images acquired on nonmydriatic eyes of subjects >50 years old with and without ocular disease using a prototype widefield (WF) slit-scanning ophthalmoscope (SSO) (ZEISS, Dublin, CA) and two standard commercial nonmydriatic fundus cameras.

**Methods:** 18 nonmydriatic eyes of 9 subjects >50 years of age were imaged using a ZEISS prototype WF SSO with the macula centered. The system acquires 90° FOV images as measured from the cornea. Comparison 45° FOV images were acquired using standard commercial nonmydriatic fundus cameras, VISUCAM® 524 (ZEISS, Jena, Germany) and VISUCAM®PRO NM (ZEISS, Jena, Germany). 8 subjects had type 2 diabetes, 2 eyes had cataracts, and 2 eyes were pseudophakic. Image quality was evaluated by a licensed optometrist. Images were graded as unusable if 1) image artifacts disrupted the ability to evaluate the central 45° FOV or 2) the size of a subject's pupil prevented the acquisition of a 45° FOV. Evidence of pathology observable in the outer 45° of the WF SSO images was recorded.

**Results:** Of the nonmydriatic eye images acquired using the prototype WF SSO, 100% (18/18) had usable image quality. Only 67% (12/18) of the nonmydriatic eye images acquired using VISUCAM 524 and VISUCAM$^{PRO\ NM}$ had usable image quality, with the rest graded as unusable because the pupil size was too small. Only a small pupil mode 30° FOV image could be acquired using VISUCAM 524 and VISUCAM$^{PRO\ NM}$. For one nonmydriatic eye image, a hemorrhage was observable in the outer 45° of the WF SSO image. Neither VISUCAM 524 nor VISUCAM$^{PRO\ NM}$ captured this hemorrhage as it was located outside the 45° FOV.

**Conclusions:** The ZEISS WF SSO is able to acquire high-quality, WF images of nonmydriatic eyes in subjects >50 years old. Though additional testing is required, the Zeiss WF SSO appears to perform at least as well as the standard 45° fundus cameras when evaluating subjects with diabetes, and may provide additional diagnostic information when pathology lies outside the 45° FOV.

Nonmydriatic right eye image of a 67 year old subject acquired using a (Left) prototype WF SSO, (Center) VISUCAM 524, and (Right) VISUCAM$^{PRO\ NM}$.

**Commercial Relationships: Jennifer Luu**, Carl Zeiss Meditec, Inc. (E); **Conor Leahy**, Carl Zeiss Meditec, Inc. (E); **Mary K. Durbin**, Carl Zeiss Meditec, Inc. (E)

**Program Number:** 5456 **Poster Board Number:** B0613
**Presentation Time:** 8:30 AM–10:15 AM

## Comparison of Usable Image Area Acquired on Nonmydriatic Eyes Using a Widefield Slit-Scanning Ophthalmoscope and Commercial Fundus Cameras

*Nathan D. Shemonski, Jennifer Luu, Abouzar Eslami, Gary C. Lee, Conor Leahy, T K. Brock*. R&D, Carl Zeiss Meditec, Inc., Dublin, CA.

**Purpose:** To compare the usable image area acquired on nonmydriatic eyes of subjects with and without ocular disease using a prototype widefield (WF) slit-scanning ophthalmoscope (SSO) (ZEISS, Dublin, CA) and two standard commercial nonmydriatic fundus cameras, VISUCAM® 524 (ZEISS, Jena, Germany) and VISUCAM®PRO NM (ZEISS, Jena, Germany).

**Methods:** Eighteen (18) nonmydriatic eyes of 9 subjects over 50 years of age were imaged using a ZEISS prototype WF SSO with the macula centered. The system acquires images that subtend a 90° FOV as measured from the cornea. Comparison images were acquired using standard commercial nonmydriatic fundus cameras, VISUCAM 524 and VISUCAM$^{PRO\ NM}$. Both VISUCAM 524 and VISUCAM$^{PRO\ NM}$ acquire images that subtend a 45° FOV. Eight (8) subjects had type 2 diabetes mellitus, 2 eyes had cataracts, and 2 eyes were pseudophakic. The usable image area was evaluated by an expert grader. Regions determined to be poor/unusable in image quality were marked and the remaining portion of the image was defined as usable. For the WF SSO system, the known image distortion was used to convert from area in pixels to area in mm$^2$. VISUCAM 524 and VISUCAM$^{PRO\ NM}$ were assumed to be distortion free when converting from pixels to area in mm$^2$.

**Results:** The usable image area for each device is summarized in Table 1 and Figure 1. For all 18 eyes, the average usable area for WF SSO was 327 mm$^2$, for VISUCAM 524 was 68.5 mm$^2$, and for VISUCAM$^{PRO\ NM}$ was 60.6 mm$^2$.

**Conclusions:** The ZEISS WF SSO provides a larger usable image area than both VISUCAM 524 and VISUCAM$^{PRO\ NM}$ for nonmydriatic eyes.

| | WF SSO | VISUCAM 524 | VISUCAM$^{PRO\ NM}$ |
|---|---|---|---|
| Number of eyes | 18 | 18 | 18 |
| Average usable area (mm$^2$) | 327 | 68.5 | 60.6 |
| Standard deviation of usable area (mm$^2$) | 139 | 44.9 | 47.2 |

Table 1 - Summary of usable image area for WF SSO, VISUCAM 524, and VISUCAM$^{PRO\ NM}$.

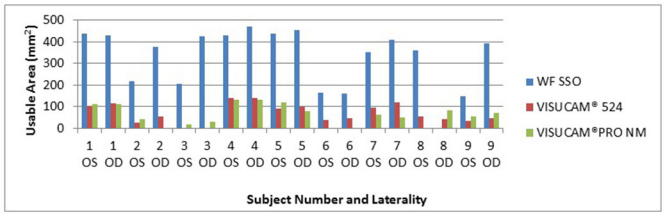


Figure 1 - Comparison of usable image area in 18 eyes (9 subjects) for WF SSO, VISUCAM 524, and VISUCAM$^{PRO\ NM}$.

**Commercial Relationships: Nathan D. Shemonski**, Carl Zeiss Meditec, Inc. (E); **Jennifer Luu**, Carl Zeiss Meditec, Inc. (E); **Abouzar Eslami**, Carl Zeiss Meditec, Inc. (E); **Gary C. Lee**, Carl Zeiss Meditec, Inc. (E); **Conor Leahy**, Carl Zeiss Meditec, Inc. (E); **T K. Brock**, Carl Zeiss Meditec, Inc. (E)

**Program Number:** 5457 **Poster Board Number:** B0614
**Presentation Time:** 8:30 AM–10:15 AM
**Imaging of Pseudophakic Eyes Using a Widefield Slit-Scanning Ophthalmoscope**
*Matthew J. Everett, Jennifer Luu, T. K. Brock, Conor Leahy, Jeff Schmidt*. Carl Zeiss Meditec, Inc., Dublin, CA.
**Purpose:** To evaluate the performance of a prototype widefield (90°) slit-scanning ophthalmoscope in undilated imaging of pseudophakic eyes.
**Methods:** True Color 90° fundus images were acquired on undilated (nonmydriatic) eyes of pseudophakic subjects using a prototype widefield (WF) slit-scanning ophthalmoscope (SSO) (ZEISS, Dublin, CA) and commercial fundus cameras. Differences in the imaging between the various fundus imagers were evaluated, with a particular focus on the ability to avoid artifacts associated with reflexes from the intraocular lens (IOL).
**Results:** Initial True Color images acquired from the prototype WF SSO are presented for an undilated, pseudophakic subject (Figure 1a). The WF images were found to be impervious to IOL artifacts, while careful patient alignment was required to avoid IOL artifacts with the commercial fundus camera (Figure 1b).
**Conclusions:** The prototype WF SSO is capable of acquiring true color 90° fundus images in undilated, pseudophakic eyes without the need for careful patient alignment to avoid IOL artifacts, in contrast to the commercial fundus camera. Further improvement in reflex minimization in the prototype is expected, along with comparison to additional commercial fundus imagers.

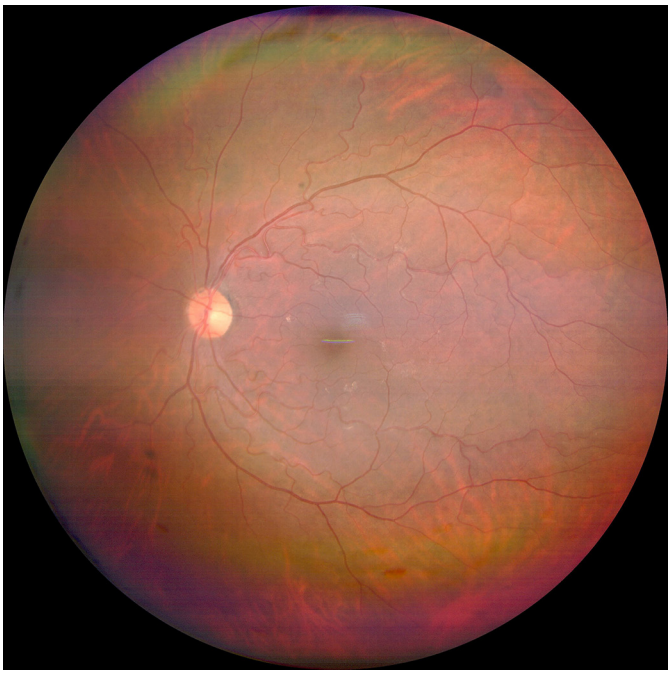

Figure 1a:
Image of nonmydriatic Pseudophakic Eye 1 acquired using a prototype WF SSO.

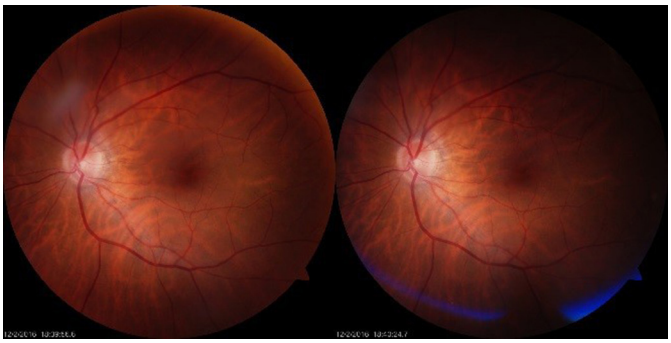

Figure 1b:
Image of nonmydriatic Pseudophakic Eye 2 acquired using a commercial fundus camera. (Right) IOL artifact is visible in image, but (Left) IOL artifact can be avoided with careful patient alignment.
**Commercial Relationships: Matthew J. Everett**; **Jennifer Luu**, Carl Zeiss Meditec, Inc. (E); **T. K. Brock**, Carl Zeiss Meditec, Inc. (E); **Conor Leahy**, Carl Zeiss Meditec, Inc. (E); **Jeff Schmidt**, Carl Zeiss Meditec, Inc. (E)

**Program Number:** 5458 **Poster Board Number:** B0615
**Presentation Time:** 8:30 AM–10:15 AM
**Revisiting oral fluorescein angiography with an ultra-wide field scanning laser ophthalmoscope; a case series from clinical practice**
*Nicole Lemanski[1, 2], Brian Lemanski[1, 3]*. [1]Ophthalmology, Mabel MP Cheng MD, PLLC, Niskayuna, NY; [2]Ophthalmology, Albany Medical Center, Albany, NY; [3]Division of Applied Vision Research, Mabel MP Cheng MD, PLLC, Niskayuna, NY.
**Purpose:** Intravenous fluorescein angiography (IV FA) is considered the gold standard in visualizing retinal vasculature. However, the complications of injection combined with potentially adverse side effects limit more widespread use in general practice. In the past, oral fluorescein angiography (OFA) has been examined as a potential alternative, but poor image quality and late phase only angiography were limiting factors. Recent advancements in modern laser based fundus photography systems have the potential to increase the clinical usefulness of OFA.
**Methods:** Retrospective analysis of 25 patients that received OFA was conducted. Age range: 25-91 years. Weight range: 150-330 lbs. Exclusions: pregnant or breast feeding patients and those with phenylketonuria or soy allergy. Patients were dilated with 1% tropicamide. After obtaining informed consent, weight and blood pressure readings, patients were given the option of sugar free liquid versus capsular formulations of sodium fluorescein (NaF), at a dose of 25-30 mg/kg, based on previous literature. After NaF, patients were photographed via ultra-wide field laser scanning ophthalmoscope (UWF-SLO) every 2 min for 30 min.
**Results:** Time from ingestion to first observable fluorescein ranged from 2-12 min. Eighty five percent of the patients showed observable fluorescence at 8 min, with a max at 15-22 min. Choroidal flush was not observed in OFA. Early, mid and late phases were observed in 90% of patients. Capsular formulation increased time in all phases. Patients weighing over 250 lbs showed decreased contrast on angiogram. There were no allergic reactions. Most common complaint was temporary dysgeusia.
**Conclusions:** OFA is a simple and effective alternative to IV FA. Longer transit times allow for bilateral panning UWF-SLO photos to be obtained by even a novice photographer. Costs are similar but OFA does not require a nurse or physician for administration. Elimination of needles, infectious waste and potential for injury, along with

painless administration and low incidence of allergic reaction make OFA appealing. To our knowledge this is the first time a sugar free mix has been used for OFA. While variations in contrast relative to weight need optimization, this preliminary study demonstrates that OFA is a good in office diagnostic tool and has potential to be used as a screening tool.

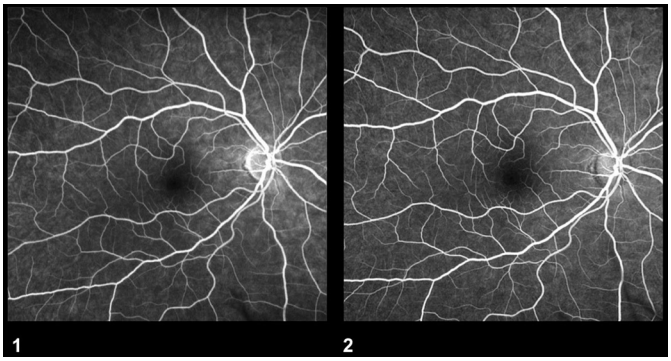


Comparison of OFA (1) vs. IV FA (2).

**Commercial Relationships: Nicole Lemanski**; **Brian Lemanski**, Nidek (F)

**Program Number:** 5459 **Poster Board Number:** B0616
**Presentation Time:** 8:30 AM–10:15 AM

**Choroidal vascular abnormalities by UWF ICGA in central serous chorioretinopathy**

*Min Sagong[1], Donghyoun Noh[1], Jano V. Hemert[2], Junyeop Lee[1], Jang Hwan Ahn[1], Jehwi Jeon[1], Junhyuk Son[1], Sooncheol Cha[1].*
[1]Department of Ophthalmology, Yeungnam University College of Medicine, Daegu, Korea (the Republic of); [2]Optos Plc, Dunfermline, United Kingdom.

**Purpose:** To evaluate vortex vein engorgement and choroidal vascular hyperpermeability in patients with central serous chorioretinopathy (CSC) using ultra-widefield indocyanine green angiography (UWF ICGA).

**Methods:** Twenty two patients with unilateral (19 patients) or bilateral (3 patients) CSC were consecutively included and imaged by UWF autofluorescence, fluorescein angiography and ICGA, and spectral domain optical coherence tomography (OCT). The number of quadrant of vortex vein engorgement was evaluated in the early phase of ICGA, which was classified as effective if the dilated choroidal vessels affect the macula. The area of choroidal vascular hyperpermeability was quantified in the late phase using by stereographic projection method. And they were correlated with clinical findings and OCT features.

**Results:** In all affected eyes, choroidal hyperpermeability from dilated choroidal vessels was observed in association with 1 or more engorged vortex vein. Affected eyes showed significantly greater choroidal hyperpermeability area ($P < 0.001$) and thicker subfoveal choroidal thickness ($P = 0.022$) compared with unaffected eyes although both eyes in the patients with unilateral CSC demonstrated symmetry of vortex congestion (78.1%). The choroidal vascular hyperpermeability was significantly correlated with subfoveal choroidal thickness ($P$=0.012, rho=0.493) and the height of subretinal fluid ($P$=0.012, rho=0.514). The number of quadrant of the effective vortex vein engorgement was correlated with subfoveal choroidal thickness ($P$=0.010, rho=0.505).

**Conclusions:** UWF ICGA could demonstrate vortex vein engorgement and choroidal vascular hyperpermeability, suggesting outflow congestion as a potential contributor to the pathogenesis of CSC. And they may serve as diagnostic clues or even predictors of disease course.

**Commercial Relationships: Min Sagong**, None; **Donghyoun Noh**, None; **Jano V. Hemert**, None; **Junyeop Lee**, None; **Jang Hwan Ahn**, None; **Jehwi Jeon**, None; **Junhyuk Son**, None; **Sooncheol Cha**, None